On-Line Speed Control of the Shunt-Connected DC Motor Via a Neurocontroller

Ruben Tapia*, Julio C. Rosas †, Omar Aguilar*, Alejandro Templos*

**Universidad Politécnica de Tulancingo, México, Ingenierias #100, Tulancingo, Hidalgo,*
ruben.tapia,[omar.aguilar]@upt.edu.mx, †Universidad Panamericana Campus Gdl, México, jrosas@gdl.cinvestav.mx

Keywords: Neurocontroller, DC motor control, neural networks.

Abstract

This paper presents the speed neural control of a shunt-connected DC motor. The rotor speed of the DC motor can follow an arbitrarily selected reference. The purpose is to achieve accurate reference control of the speed, especially when motor and load parameters are unknown. For this task, an on-line B-spline neural network is proposed due to its simple structure, adaptability, and robustness, taking into account the unknown nonlinear dynamics of the DC motor and load. Laboratory tests demonstrate the applicability of the proposition compared with the conventional PI control scheme. The performance of the resulting system has been tested on a 120 V, 2.8 A, 188.49 rad/sec DC motor.

1 Introduction

Traditionally motor control systems have contained only electromechanical components, where all connections are hardwired. Even today, these components remain the workhorses of control systems, but advances in solid-state technology and intelligent devices have allowed the emergence of equipment that could be programmed to do more than just turn a motor on and off. Such components include variable-frequency drives, solid-state starters, and electronic-overload relays [1-3]. The integration of software and intelligent devices into motor control systems can deliver improved diagnostics, early warnings for increased system reliability, design flexibility, and simplified wiring [4-6]. Such benefits can help to reduce maintenance costs and prevent unscheduled downtimes for electrical drive systems.

There are some rotational mechanical loads, which require a wide range of operating speeds. Suitable operating characteristics to provide a given range of load torques and speeds might be provided by several forms [1-5, 7]. However, they are mainly focused on conventional linear control schemes, for instance the PI control design based on a linearized model, which cannot guarantee its performance under diverse operating conditions.

The use of artificial neural networks (ANNs) offers an attractive alternative for the DC motor control. The ANNs are able to model and control on-line nonlinear and non-stationary systems. The ANNs' nature makes them robust, adaptive, optimum, and hybrid control techniques, with attractive features to motor systems control [8-9]. At the same time, the control techniques must consider the complexity of practical systems, and to provide a realistic control model with less computation time for effective robust control over a wide range of operating conditions. The B-spline neural networks offer all of them characteristics. In this paper a B-Spline Neural Network (B-SNN) is employed for the rotor speed control in face of load and speed changes.

This paper is organized as follows; section II presents the motor dynamic model. In section III, a brief description of the identification parameters of DC motor is exposed. B-spline neural network and the control strategy are discussed in section IV. Section V summarizes the laboratory implementation and VI the obtained results compared with conventional PI control, on a shunt-connected DC motor.

2 Motor Dynamics

An equivalent circuit diagram of the DC motor (shunt connected) driving a three-phase generator is shown in Figure 1. The voltage and mechanical equilibrium equations are as follows,

$$v_f = R_f i_f + L_f \frac{di_f}{dt} \qquad (1)$$

$$v_a - e_a = R_a i_a + L_a \frac{di_a}{dt} \qquad (2)$$

$$T_e = J \frac{d\omega}{dt} + T_L + B\omega \qquad (3)$$

where ω is the rotor speed, rad/sec; J is the moment of inertia, kg.m^2; R_a and R_f are the armature and field resistances, Ω; L_a and L_f are the armature and field inductances, H; i_a and i_f are the armature and field currents, A; $v_a = v_f$ is the motor's armature voltage, V; e_a is the back emf, V; T_e is the electric torque, N.m; B is the viscous friction coefficient, N.m.s; T_L is the load torque.

The back emf can be expressed proportionally to speed,

$$e_a = k_a \omega \qquad (4)$$

where k_a is the armature constant, and is related with the motor's physical properties, for instance, magnetic field strength, number of coils, etc., [2]. The electrical torque becomes

$$T_e = k_a i_a \qquad (5)$$

It is assumed that the magnetic field is constant and proportional to the field current; thus

$$k_a = L_{af} i_f \qquad (6)$$

L_{af} is the mutual inductance between the field and armature windings, H.

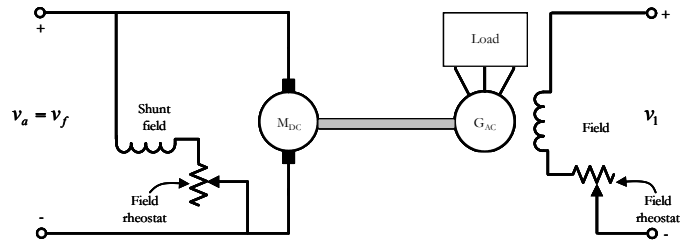

Figureure 1. Equivalent circuit diagram of the DC motor.

Equations (1)-(6) describe the DC motor behaviour and have been used to estimate the machine parameters. The mathematical model is employed for analysing and simulating the proposed neural control strategy.

3 Parameters Estimation

The major motor parameters to estimate are the armature and field resistances, the armature and field inductances, the moment of inertia, and the mutual inductance. The following procedure has been employed to evaluate them.

The nominal values of the motor under study are: 120 V, 2.8 A, and 188.49 rad/sec. The motor is loaded by an AC three-phase generator whose nominal values are: 120 V, 0.33 A and 188.49 rad/sec, where a balanced three-phase resistive load is connected, Figure. 1.

Firstly, the voltage and current measurement at full load is accomplished, given the following information

$$v_a = v_f = 111.8 \text{ V}, \qquad i_a = 1.22 \text{ A}$$
$$i_f = 0.238 \text{ A}, \qquad \omega = 1800 \text{ rpm}$$

To calculate the resistances of both windings it is assumed that the motor has two DC circuits (field and armature) feed by one DC source connected through a series resistance. Thus, such parameters can estimated by measuring individually the voltage and current on each winding, under different applied DC voltage values, and then fulfilling an extrapolation of the resulting values to estimate the best ones. The rheostat field is included into the resistance of the field winding. The maximum voltage applied to the armature winding is such that the nominal current, 2.8 A, is drawn. Thus, the following parameters result

$$R_f = \frac{v_f}{i_f} = 469.7479\ \Omega, \qquad R_a = \frac{v_a}{i_a} = 7.5\ \Omega$$

Similarly, to evaluate the armature and field inductances, two circuits are taking into account, although in this case they are feed by an AC source. The above procedure is repeated for obtaining the values of the inductances; in this case, both magnitudes and phase between the AC voltage and current signals are measured, and then the following relationships are utilized,

$$\tan\theta = \frac{X}{R}, \qquad Z = R + jX \qquad (7)$$

where θ is the shift phase between the sinusoidal voltage and current waveforms present in the AC circuit; Z is the impedance in Ω; R is the resistance in Ω; and X is the reactance en Ω. It is assumed that the resistance R is available from the above-mentioned results. For the inductive circuit the inductance is defined as,

$$X_L = 2\pi f L \qquad (8)$$

If the shift angle and resistance are known, the inductance can be evaluated from Equations (7)-(8). Therefore,

$$L_f = 2.4080 \text{ H}, \qquad L_a = 55.3 \text{ H}$$

The mutual inductance, L_{af}, is estimated through the steady state measurements related with Equations (2)-(6), becoming

$$L_{af} = 2.2881 \text{ H}$$

To establish the moment of inertia, J, first the inertia constant in seconds, H, is calculated under the following swing equation approximation [2-3]

$$H = \frac{-P_m}{\Delta\omega/\Delta t} \qquad (9a)$$

where H is defined as

$$H = \frac{\frac{1}{2} J\omega^2}{S_B} \qquad (9b)$$

being S_B the nominal motor power in VA, and ω is the nominal speed in rad/sec.

To infer the slope $\Delta\omega/\Delta t$, we propose to approximate this value by mean of the measured velocity when the voltage is disconnected with the motor at full load. Figure 2 depicts the measured speed evolution; both motor's and generator's inertias are included. The measurement is employed to evaluate the slope in a least-squares sense. Applying the motor values previously obtained,

$$J = \frac{-P_m S_B}{\Delta\omega/\Delta t \; \frac{1}{2}\omega^2} = 0.0013 \text{ kg.m}^2$$

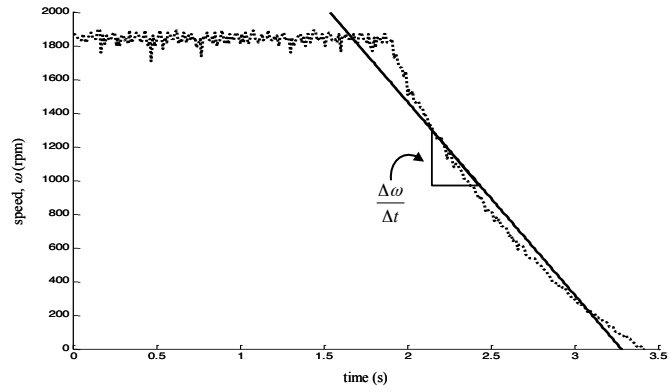

Figure 2. Motor speed evolution at full load. The voltage is disconnected at t = 1.91 s.

Therefore, the motor parameters are estimated by the above mentioned procedure, and they have been used for studying the system control performance before the neurocontroller is built.

4 Neurocontroller

The output power developed by a DC motor is proportional to the product of the shaft torque and the shaft rotational speed. The value of the developed torque usually varies automatically to satisfy the demand of the load torque plus any torque associated with friction and wind age. The increment of the shaft power due to the load torque increment is usually supplied by an automatic increase of the motor's current. Any significant change in motor speed, however, must be obtained in a controlled manner by making some adjustment to the motor or to its electrical supply. Within limits, as can be seen from Equations (1)–(5), the operating speed of a shunt-connected DC motor may be controlled in a straightforward manner by varying the armature voltage v_a.

In the following, the operating speed of the shunt-connected DC motor is controlled by modulating voltage, v_a. The voltage control system is based on a PWM scheme, where the control signal is α, Figure 3.

Thus, an adaptive control law which considers the nonlinear nature of the plant and load, and that can be adapted to the changes in the environment and parameters is required for regulating the motor velocity. Therefore, in this paper a B-spline neural control is proposed.

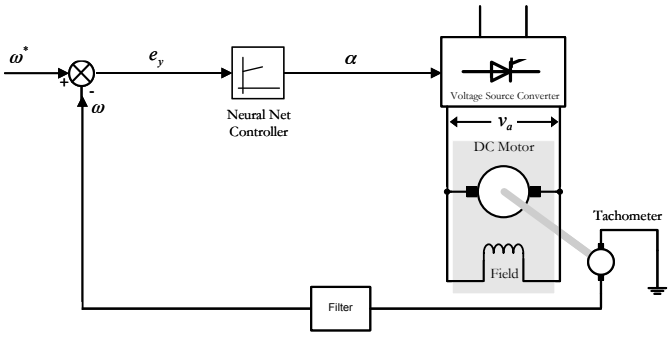

Figure 3. Speed control loop of the shunt-connected DC motor

The B-spline neural networks (B-SNN) are a particular case of neural networks that allow to control and model systems adaptively, with the option of carrying out such tasks on-line and taking into account the system non-linearities. Additionally, through B-SNN there is the possibility to bound the input space by the basis functions definition.

The input space of this type of ANN is normalized by a lattice on which the basis functions are defined. Only a fixed number of basis functions participate in the network's output; and then not all the weights have to be calculated each time step, thus reducing the computational effort and time [10].

The controller provides a suitable voltage to the armature through a B-spline neural net. With this purpose, the input signal e_y is utilized for controlling v_a, Figure 4. The B-SNN output can be described by,

$$y = \boldsymbol{a}^T \boldsymbol{w} \qquad (10)$$

and

$$\boldsymbol{w} = [w_1\ w_2\ ]^T, \qquad \boldsymbol{a} = [a_1\ a_2\ ]^T$$

where w_i y a_i are the i-th weight and the i-th B-SNN basis function output, respectively.

In this paper, the neurocontroller is constituted by two basis functions, Figure 4. The error, e_y, between the reference speed and the actual, is the input for controlling v_a.

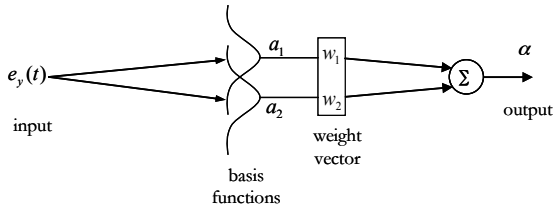

Figure 4. Proposed B-SNN controller.

In order to define a lattice of the input space, a set of M knot vectors must be specified, one knot vector for each input axis. These knot values give the positions of the (M-1)-dimensional hyperplanes which are parallel to the other (M-1) axes, and the set of all the hyperplanes generates the lattice in the input space. There are usually a different number of knots on each axis and they are generally placed at different positions. More specifically, a knot vector must be specified for each input axis, and consists of interior and exterior knots. Given a knot vector, Fig 5, we can define a univariate basis function. For more details in modelling and control systems with B-spline neural networks see [10-11].

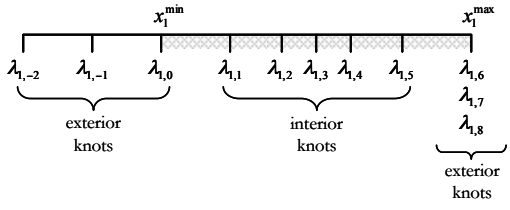

Figure 5. A knot vector on a one-dimensional input space.

The neurocontroller, Equation (10) is created by two univariate basis functions of order 3, considering that e_y is bounded within [-6.0, 6.0], Figure 6.

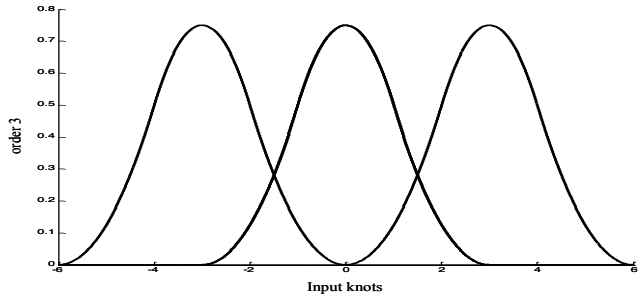

Figure 6. Univariate B-spline basis functions of order 3.

In this paper, the neurocontroller is trained on-line using the following error correction instantaneous learning rule [10]

$$w_i(t) = w_i(t-1) + \frac{\eta\, e_y(t)}{\|\boldsymbol{a}(t)\|_2^2} a_i(t) \qquad (11)$$

where: η is the learning rate and $e_y(t)$ is the instantaneous output error.

The learning rate has to be tuned for obtaining a smooth response and its value can be: $0 < \eta < 2$, resulting from an autocorrelation matrix analysis, [10]. The learning is stable if and only if the learning rate satisfies the previous condition. The basis functions are defined from the knot vector considering the input bound, and the order due to the network's output become smoother as the order increases.

The instantaneously trained neural networks possess generalization characteristics [12]. An instantaneously trained neural network must, by definition, convert the incoming pattern into corresponding weights without intensive computations. Therefore, B-spline neural networks offer an attractive alternative and in this paper are implemented with continuously on-line trained, Equation (11), for controlling the DC motor speed.

5 Laboratory Implementation

The speed measurement is made via a tachometer, and the instantaneous value is captured using the microcontroller MC68HC908QY4CP, who communicates with the computer. Manipulation of the armature voltage, v_a, is performed through an adjustable source that is constructed by insulated gate bipolar transistors (IGBTs). To reduce the high frequency harmonics of the pulse width modulation, (PWM) scheme low pass filter is added at the source side. The schemes based on pulse width modulation are widely used in the handling of voltage source converter through proper management of power electronic switches.

The strategy is based on PWM technique, that pulses are low power signals from a controller. In this work, a digital PWM is used, so that the voltage of the pulses is maintained constant during the change in pulse width.

The PWM comparator is constructed by generating the signal handling switches. The comparator sends a signal to close the switch when the modulated signal (sinusoidal signal) is larger than the carrier otherwise the switches are open. In this case, the carrier signal is triangular, and the frequency of the PWM depends the modulated signal, which acts as a reference signal.

Therefore, the PWM control strategy is implemented by a microcontroller, where the control signal is generated using a B-spline neural scheme which keeps the armature voltage on the courage to take engine speed at the desired reference value, Figure 3.

6 Test Results

In order to evaluate the speed regulation, digital simulations and laboratory tests are accomplished using the DC motor arrangement described in Figure 1, under different disturbances.

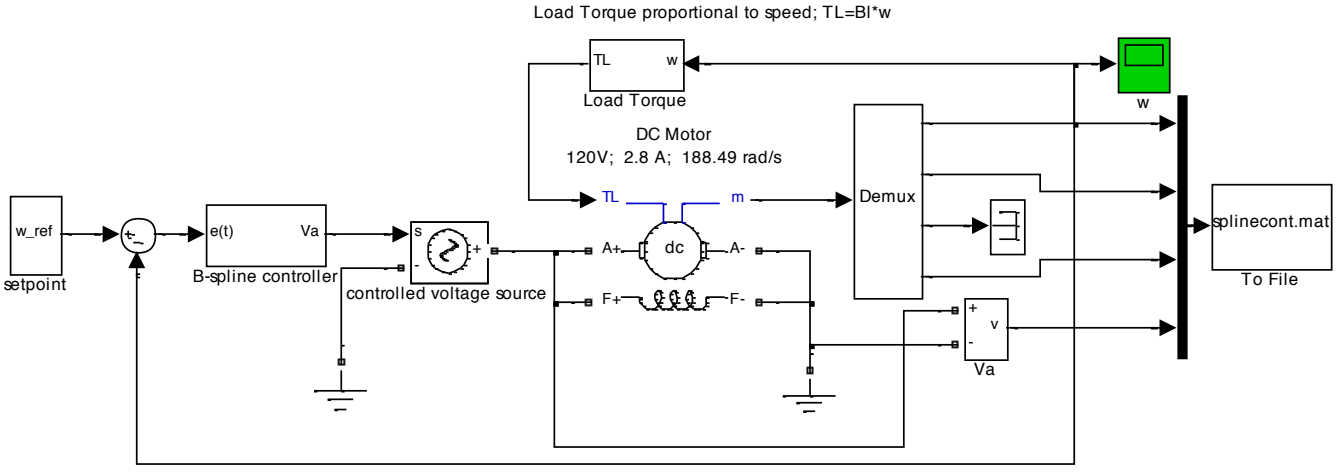

Figure 7. DC motor control scheme by B-spline controller.

The following scenarios are included: a) simulation with B-SNN controller (NNC-M); b) laboratory tests with B-SNN controller (NNC); c) laboratory tests with conventional PI control (CONV). The Matlab-Simulink® is employed for simulating. For simplicity the load in simulation study is represented proportional to velocity as

$$T_L = B_L \omega$$

where the constant B_L is calculated by trial and error procedure, considering the current and voltage measured in laboratory tests in steady state with different load values. Figure 7 displays the DC motor control system model controlled by the B-spline neural networks.

To study the proposed controller analyzes three cases, when the reference value is changed, Figure 8. Figure 9 shows the performance of the speed when the load is switched off, and finally, in Figure 10 is seen the speed evolution when the load is reconnected.

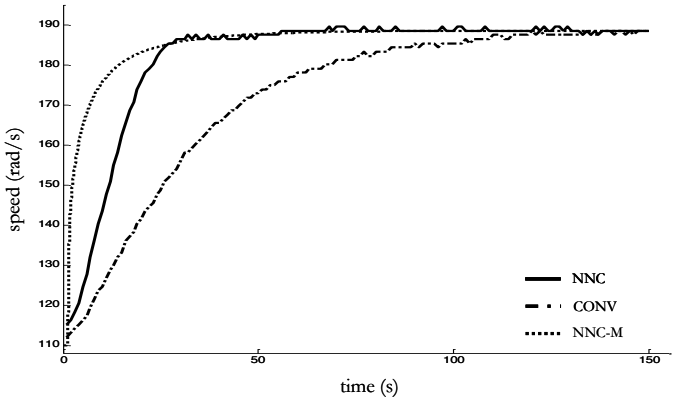

Figure 8. Tracking performance for starting DC motor from 110 to 188.49 rad/s.

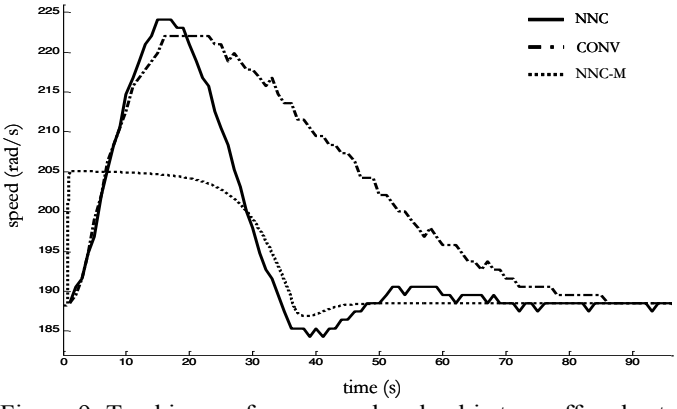

Figure 9. Tracking performance when load is turn off and set point is 188.49 rad/s.

The NNC has the ability of being updated to a new operating condition, improving the CONV performance. In contrast to the NNC, the CONV control technique has a slower response. Discrepancies with simulations are due to a rough estimation of parameters.

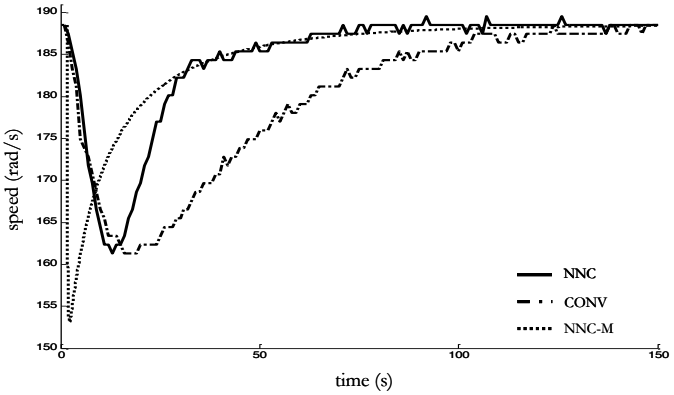

Figure 10. Tracking performance when load is turn on and set point is 188.49 rad/s.

The performance and applicability of the proposition are proved by hardware implementation on a laboratory DC motor. This strategy allows controlling appropriately the motor speed where the load and set point is modified.

The NNC and CONV scenarios are compared and can be concluded that, while the neural control is able to adapt by itself to different operating conditions, the performance of the CONV turns out to be diminished in some situations, especially under different operating conditions for which its parameters have been tuned. Thus, the feedback signals to the NNC are pertinent for a suitable control of the DC motor (shunt connected) velocity exhibiting a well performance for different operating points without modifications in control law.

Acknowledgements

This work was supported by PROMEP: Redes Temáticas de Colaboración under the project titled: Fuentes de Energías Alternas.

References

[1] W. Shepherd, L.N. Hulley and D.T.W. Liang, “Power Electronics and motor control,” Cambridge University Press, 1995.

[2] A. E. Fitzgerald, Jr., Charles Kingsley, Stephen D. Umans, “Electric Machinery”. McGraw-Hill, 2003.

[3] Chee-Mun Ong, “Dynamic Simulation of Electric Machinery,” Prentice Hall, 1998.

[4] Francisco Beltran-Carbajal, Antonio Favela-Contreras, Antonio Valderrabano-Gonzalez, Julio Cesar Rosas-Caro, “Output feedback control for robust tracking of position trajectories for DC electric motors”, Electric Power Systems Research, **volume** 107, pp. 183-189, (2014).

[5] R. Morales, J.A. Somolinos, H. Sira-Ramírez, “Control of a DC motor using algebraic derivative estimation with real time experiments”, Measurement, **volume** 47, pp. 401-417, (2014).

[6] Hajiaghajani, M.; Toliyat, H.A.; Panahi, I.M.S., “Advanced fault diagnosis of a DC motor,” IEEE Trans. Energy Conversion, **volume** 19, No. 1, pp. 60–65,

(2004).
[7] Crnosija, P., Krishnan, R., Bjazic, T., "Transient performance based design optimization of PM brushless DC motor drive speed controller," Proceedings of the IEEE International Symposium on Industrial Electronics, ISIE, **volume** 3, pp. 881-886, (2005).
[8] Gerasimos G. Rigatos, "Adaptive fuzzy control of DC motors using state and output feedback", Electric Power Systems Research, **volume** 79, No. 11, pp. 1579-1592, (2009).
[9] Jian Sun, Yi Chai, Chunxiao Su, Zhiqin Zhu, Xianke Luo, "BLDC motor speed control system fault diagnosis based on LRGF neural network and adaptive lifting scheme", Applied Soft Computing, **volume** 14, pp. 609-622, (2014).
[10] Brown, and C. Harris, *Neurofuzzy Adaptive Modelling and Control*, Prentice Hall International, 1994.
[11] Rubén Tapia O. and Juan M. Ramírez, "Power Systems Neural Voltage Control by a StatCom", Proceedings of the IEEE World Congress on Computational Intelligence, Vancouver, Canadá, 2006.
[12] K.W. Tang, "Instantaneous Learning Neural Networks," Ph.D. Dissertation, LSU, 1999.